## ABSTRACT

The aspirating probe originally designed by Epstein and Ng at MIT was modified by replacing the two platinum coated tungsten hot wires normally used with platinum iridium alloy wires. The resulting improved unsteady total pressure and total temperature resolution of the modified probe is demonstrated. Flowfield measurements were made downstream of NASA Rotor 37 for a part speed operating condition to test the performance of the probe. Time resolved blade-to-blade total temperature and total pressure as calculated from the two platinum iridium hot wire voltages are shown. The flowfield measurements are compared with independent measurements of total pressure with high response transducers and total temperature calculated from laser anemometer measurements. Limitations of a more often used unsteady temperature data reduction method which involves only one aspirating probe hot wire voltage and a high-response pressure measurement are discussed.


## NOMENCLATURE

| | |
|---|---|
| $A^*$ | throat area at sonic orifice |
| $A_c$ | channel area at wire plane |
| $R_s$ | series resistance of anemometer |
| $R_w$ | resistance of a hot wire at operating temperature |
| V | anemometer bridge voltage |
| $\gamma$ | ratio of specific heats |
| R | gas constant for air |
| U | fluid velocity in choked channel |
| $\rho$ | density of air |
| $P_T$ | total pressure of fluid being measured |
| $T_T$ | total temperature of fluid being measured |
| $T_w$ | wire operating temperature |
| l | hot wire length |
| d | hot wire diameter |
| r | ratio of static to total temperature of fluid being measured |
| $\kappa$ | fluid thermal conductivity |
| Nu | Nusselt number |
| C,n | hot wire calibration constants |

## INTRODUCTION

The accurate measurement of the aerodynamic performance parameters for flow through an axial-flow, transonic compressor stage is still an important engineering problem. The three-dimensionality, compressibility, and unsteadiness of transonic compressor stage flow can contribute to fluid temperature, pressure, and velocity measurement errors that result in a significant misrepresentation of rotor and stage efficiency.

The aspirating probe invented by researchers at MIT (Ng and Epstein, 1983) is intended to be a tool for accurately measuring time-resolved total temperature and total pressure in compressor flows. However, personal experience with this probe revealed serious limitations. Some of these limitations have been overcome with a simple improvement involving a change in hot-wire material.

The main objective of this paper is to share details about the improved aspirating probe with readers who may be interested in using the aspirating probe as it was originally intended.

## ASPIRATING PROBE

The voltage, V, required to maintain a conventional hot wire at a constant temperature, $T_w$, is a function of the wire-to-fluid temperature difference, $(T_w - rT_T)$, and fluid mass flux, $(\rho U)$, at the wire plane. The functional relationship is:

$$V^2 = f(\rho U)(T_w - rT_T) \tag{1}$$

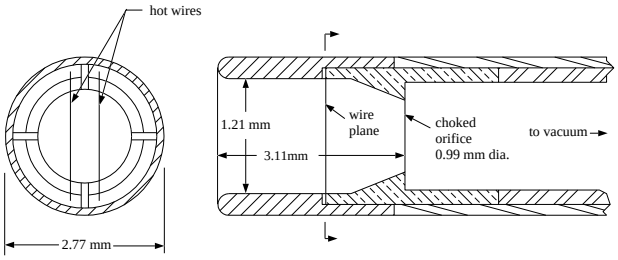


FIGURE 1 Schematic of aspirating probe.

In an unsteady compressible flow, $\rho, U, T,$and $P$ all fluctuate with time making the hot wire data extremely difficult to interpret. To overcome this difficulty, Ng and Epstein (1983) placed a pair of co-planar hot wires operating at different overheat ratios in a channel whose exit is choked. Figure 1 is a schematic of this channel.

The continuity equation for one-dimensional channel flow at the sonic orifice is

$$(\rho U)^* = \left(\frac{P_T}{\sqrt{T_T}}\right)\sqrt{\frac{\gamma}{R}}\left(\frac{2}{\gamma+1}\right)^{\frac{(\gamma+1)}{2(\gamma-1)}} \tag{2}$$

By applying mass conservation in the channel, Eqn. 2 can be written as

$$\rho U = \left(\frac{P_T}{\sqrt{T_T}}\right)\frac{A^*}{A_c}\sqrt{\frac{\gamma}{R}}\left(\frac{2}{\gamma+1}\right)^{\frac{(\gamma+1)}{2(\gamma-1)}} \tag{3}$$

which states that $(\rho U)$ is a function of free stream total pressure and total temperature. Eqn. 1 may thus be expressed as

$$V^2 = f\left(\frac{P_T}{\sqrt{T_T}}\right)(T_w - rT_T) \tag{4}$$

For a constant temperature hot wire we also have

$$V^2 = \frac{(R_s + R_w)^2}{R_w}\pi l \kappa N u (T_w - rT_T) \tag{5}$$

By equating Eqn. 4 and Eqn. 5 and grouping parameters that are fixed for a set probe geometry and gas composition into constants, the working equation for the wires becomes

$$V_i^2 = \left[C_i\left(\frac{P_T}{\sqrt{T_T}}\right)^{n_i} + D_i\right](T_{w_i} - rT_T) \tag{6}$$

where

$$C_i, n_i, D_i = f(T_T, l_{hw}, d_{hw}, N u) \tag{7}$$

The subscript $i$ refers to the hot wire number, either 1 or 2, and the constants $C_i$, $n_i$ and $D_i$ are determined from a calibration procedure. This was the version of Eqn. 6 originally derived by Ng and Epstein (1983). From his experiences in using the probe for $P_T$ and $T_T$ measurements, Dr. Ng determined that $D_i$ was negligible and he dropped it from the working equation. This


FIGURE 2 NASA1 high-response probe.

reduced formulation of Eqn. 6, with $D_i = 0$, was used by Alday and Ng (1991), Alday et al. (1993) and Van Zante (1992).

To calculate $T_T$ and $P_T$ using the two hot wire voltages, $V_1$ and $V_2$, the two simultaneous equations

$$\begin{aligned} V_1^2 &= \left[C_1\left(\frac{P_T}{\sqrt{T_T}}\right)^{n_1} + D_1\right](T_{w_1} - rT_T) \\ V_2^2 &= \left[C_2\left(\frac{P_T}{\sqrt{T_T}}\right)^{n_2} + D_2\right](T_{w_2} - rT_T) \end{aligned} \tag{8}$$

must be solved. The two hot wires in the choked channel provide two measurements from which $T_T$ and $P_T$ can be deduced using Eqn. 8 and thus form the basis for the aspirating probe design and operation. A more in-depth discussion of the aspirating probe design is available in Ng and Epstein (1983) and Ng (1983).

The independence of the two relations in Eqn. 8 will determine the probe sensitivity to $T_T$ and $P_T$ and thus the shape of the calibration space. The difference between the hot wire temperatures, $|T_{w_2} - T_{w_1}|$, influences the independence of the two simultaneous equations, thus if $T_{w_1}$ is nearly equal to $T_{w_2}$, the equations will be almost identical and therefore have limited independence. Solving these equations with limited independence is like attempting a solution represented by the intersection of two nearly parallel lines. The calibration constants are also functions of total temperature, hot wire length and diameter, etc. but these factors have a lesser effect on the independence of the equations than the wire temperatures. The greater the separation in wire temperatures, the more independent the two hot wire equations will be with improved sensitivity to temperature and pressure.

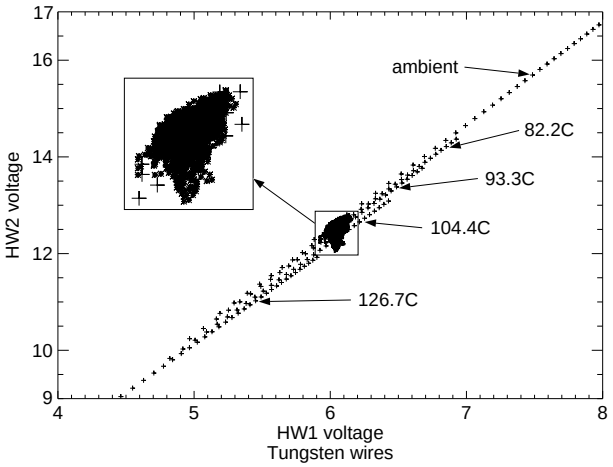


FIGURE 3 Original calibration space of aspirating probe with representative data shown.

## PERFORMANCE OF ORIGINAL PROBE

The original version of the aspirating probe used a 5 $\mu$m (0.0002 inch) diameter tungsten hot wire for channel 1 and an 8.9 $\mu$m (0.00035 inch) diameter tungsten hot wire for channel 2. The overheat ratios for the wires were 1.8 and 2.0 giving wire temperatures of 216°C (420 °F) and 263°C (505 °F) respectively.

For an independent measure of total pressure, a Kulite model XCQ-062 semiconductor pressure transducer was mounted beside the aspirating probe. To reduce thermal drift, the transducer was thermally compensated by the manufacturer as well as with an external sense resistor as described in Cherrett and Bryce (1991). Figure 2 shows a front view of the combination probe. The aspirating probe is on the left and the Kulite is on the right.

Calibrations of the aspirating probe were accomplished in a static air tank at different constant temperatures and variable pressure to determine the constants $C_i$, $n_i$ and $D_i$. Calibrations were obtained at ambient temperatures, 60.0, 71.1, 82.2, 93.3, 104.4, 116.6, and 127.7°C (140, 160, 180, 200, 220, 240, and 260 °F) at pressures from 101.4 kPa to 241.3 kPa (14.7 to 35 psia). The initial calibration procedure used is identical to that used in previous applications of the aspirating probe (Alday and Ng, 1991; Van Zante, 1992). Eqn. 6, with $D_i = 0$, was written in logarithmic form and a linear least squares routine was used to determine the calibration constants for each wire at each calibration temperature.

A set of calibration constants, $C_i$ and $n_i$, was determined for each wire for each constant temperature calibration. Figure 3 shows the calibration space for the tungsten hot wires as hot wire 1 voltage versus hot wire 2 voltage for the range of calibration temperatures and pressures. For clarity only five constant temperature lines are shown. Each line of + symbols is a constant temperature line and each + symbol represents a pressure value from 68.9 kPa (10 psia) in the lower left to 275.8 kPa (40 psia) in the upper right in increments of 6.9 kPa (1 psi).

Each constant temperature calibration line was generated from the constants derived from a calibration at that temperature. Ng (Ng and Epstein, 1983) stated that calibration constants from the ambient temperature calibration could be used to predict the probe performance at higher temperatures. For the current range of calibration temperatures and pressures, this was not the case. Therefore, with this initial calibration procedure, a more extensive calibration was needed and calibration constants were calculated for every calibration temperature.

In his application of the aspirating probe to determine $P_T$, $T_T$, and species concentration, Kotidis (1989) also followed an accurate but less time intensive calibration procedure. He used the original working equation with three constants, $C_i$, $n_i$, and $D_i$, and determined the temperature dependence of the constants. Kotidis's formulation of the probe equations was simplified to remove the species concentration dependence. Because the Kotidis formulation of the probe governing equations accounts for the temperature dependence of $C_i$, $n_i$, and $D_i$, a subset of the initial calibration data can be used to characterize the probe behavior over the same region as the initial calibration procedure. An extensive 'reference' calibration is done at room temperature. The remainder of the anticipated operating region for the probe is characterized by acquiring a series of 'random' pressure/temperature points throughout the region. Since it requires one third to one half as many calibration points, this refined calibration procedure is much less tedious and time consuming than the initial procedure. The Kotidis calibration procedure was used to generate the calibration space that was used for data reduction in this report.

The extremely narrow wedge shape of the initial calibration space in Figure 3 indicates that the sensitivity of the aspirating probe to pressure and temperature variations is poor. Very small changes in hot wire voltage correspond to large changes in temperature and pressure. The asterisks overlaid on the calibration space in Figure 3 are measurements acquired downstream of Rotor 37 at midspan at a part-speed operating condition. Several thousand measurements are shown. Since the measurements were acquired across all the blade passages, the envelope of the measurements indicates the excursions in pressure and temperature across the blade pitch as well as passage-to-passage flow non-uniformities in the rotor. The measurement envelope is large relative to the calibration space; a significant portion of the data actually lies outside of the calibration space. Because of poor probe sensitivity, the excursions of 'data' outside of the calibration space was probably due to the inability of the probe to respond correctly to the dynamic fluctuations of $P_T$ and $T_T$ in the compressor. It is not reasonable to reduce these data to total pressures and total temperatures using the two hot wire voltages because of the poor instrument sensitivity and data scatter.

To overcome this severe sensitivity limitation, total temperature was alternately calculated using the total pressure from the Kulite transducer and only one hot wire voltage from the aspirating probe as suggested by Ng and his students (Morris et al., 1992). The limitations of this data reduction method will be discussed later. Instead of combining the outputs of two different high-response instruments to measure a time-resolved temperature, a better solution is to modify the aspirating probe to improve its sensitivity so it can be used alone for this measurement.

TABLE 1 Summary of hot wire material properties.

| Type | Max $T_{ambient}$ °F (°C) | Max $T_{sensor}$ °F (°C) | Temp coef of resistance (/°C) |
|---|---|---|---|
| Tungsten | 300 (150) | 570 (300) | 0.0042 |
| Platinum iridium | 1400 (750) | 1470 (800) | 0.0009 |

As mentioned previously, the ability of the probe to follow changes in total pressure and total temperature is related to the performance of the hot-wire anemometry in the flow environment and to the independence of the simultaneous equations, Eqn. 8 for wires 1 and 2, which must be solved for $P_T$ and $T_T$.

The performance of a hot wire and anemometer is related to the wire-to-fluid temperature difference, $(T_w - rT_T)$. The total temperature downstream of Rotor 37 is significantly above ambient thus reducing the wire-to-fluid temperature difference possible with tungsten which has a limited maximum temperature. This reduces the frequency response of the wire and leads to non-linearity in the anemometer response. In a flow with temperature fluctuations, Smits et al. (1983) recommends high overheat ratios to avoid contamination of the mass flow signal from the fluctuating temperature. As ambient temperature rises, very high overheat ratios or wire temperatures are required. This is the case in an environment like the flow downstream of Rotor 37.

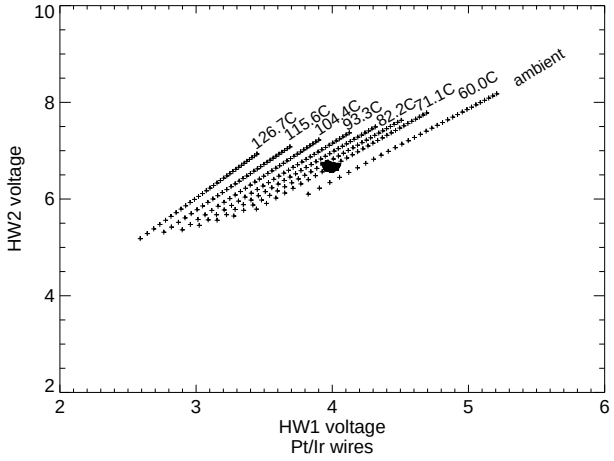


FIGURE 4 Calibration space with platinum iridium wires with representative data set shown.

## MODIFIED ASPIRATING PROBE

Because of the relatively low maximum operating temperature of tungsten hot wires, the optimum conditions of high wire temperature and significant spread between wire temperatures are out of reach for this material. Thus platinum iridium alloy wires were chosen to replace the tungsten wires. Table 1 summarizes both tungsten and platinum iridium wire properties. The platinum iridium (Pt/Ir) alloy wires allow high wire temperatures and also have a high enough maximum temperature to permit a significant spread between wire temperatures.

The tungsten wires of the original aspirating probe were replaced with 6.3 $\mu$m (0.00025 inch) diameter platinum iridium alloy wires on channels 1 and 2 of the anemometer. The operating temperatures of the wires were set to 260°C (500°F) and 371°C (700°F) for wire 1 and 2 respectively. Because of the different temperature coefficient of resistance for platinum iridium relative to tungsten, the overheat ratios were 1.21 and 1.31 respectively.

The modified probe was calibrated and the resulting calibration space is shown in Figure 4 to the same scale as the tungsten wire calibration space shown in Figure 3. All eight constant temperature lines are shown and each line represents a pressure range of 68.9 to 275.8 kPa (10 to 40 psia). A data set taken with the modified aspirating probe at conditions equivalent to the data set shown in Figure 3 is superimposed on the calibration space. The calibration space is more 'open' which allows much better resolution of total temperature and pressure. In addition, the data scatter is reduced considerably and the region of data scatter corresponds to reasonable changes in temperature and pressure.

Because of the improved performance of the modified probe, it is now possible to determine time-resolved total temperature and total pressure from the two hot-wire voltages. Also a comparison of unsteady temperature and pressure measured with the two wires and unsteady pressure and temperature measured with one wire and the Kulite can be done.

## DATA REDUCTION

Earlier data reduction methods used a single set of calibration constants and, using either both $V_1$ and $V_2$ or the Kulite pressure value and one hot wire voltage, solved Eqn. 8 ($D_i = 0$) by an iterative method. These data reduction methods assume that $C_i$ and $n_i$ are not functions of $T_T$. For the present study this was not a reasonable assumption and a more rigorous data reduction procedure was followed.

The calibration space was parameterized in terms of two independent variables, u and v, using a spline geometry subroutine package called DT_NURBS (Boeing and U.S. Navy, 1992). Two surfaces result:

$$\begin{aligned} S_1 &: \; P_T(u,v), V_1(u,v), V_2(u,v) \\ S_2 &: \; T_T(u,v), V_1(u,v), V_2(u,v) \end{aligned} \tag{9}$$

A second degree B-spline surface was interpolated through the calibration data to form each surface. Reducing the experimental data to $T_T$ and $P_T$ was done using a Newton Raphson style root finding method on the parameterized surfaces. This is a convenient

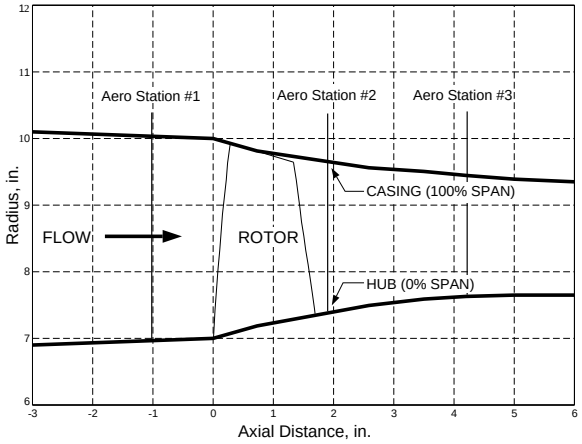


FIGURE 5 Rotor 37 flowpath and measurement locations.

TABLE 2 60% speed operating conditions.

| | |
|---|---|
| RPM | 10,300 |
| Weight flow (kg/s) | 13.7 |
| Pressure Ratio | 1.25 |
| Blade Passing Frequency (Hz) | 6,200 |
| Sampling Frequency (Hz) | 284,280 |

way of manipulating the calibration space because any data pair can be used. For example, ($V_1$,$V_2$) or ($V_1$,$P_T$) can drive the iteration procedure to find the u,v values for the third unknown, either ($P_T$, $T_T$) or $T_T$ respectively. The method is also fast, which is essential because of the large volume of data requiring reduction.

## THE EXPERIMENT

Flowfield measurements were acquired using the modified aspirating probe downstream of NASA Rotor 37 in the single stage compressor research facility at the NASA Lewis Research Center. Detailed design and aerodynamic performance data for the rotor are presented in Reid and Moore (1978) and Moore and Reid (1980). Figure 5 shows the compressor flowpath and measurement locations.

The rotor was designed for a total pressure ratio of 2.1, a weight flow of 20.2 kg/s (44.5 lb/s), and a rotor tip speed of 454 m/s (1490 ft/s) at a design speed of 17,200 rpm. For this study the rotor was operated at 60% speed, see Table 2 for an operating condition summary. Aspirating probe and high-response pressure probe measurements were acquired at the station 3 axial plane of the compressor for this part speed condition. Laser fringe anemometer measurements were acquired just upstream of station 3 at 9.4 cm (3.7 inches) axial distance.

The aspirating and pressure probe signals were digitized with a 12 bit resolution A/D system. The A/D system samples were phase-locked to the rotor by using the output pulse train of a shaft angle encoder to trigger the digitizer. The shaft angle encoder used the elapsed time between once-per-revolution (OPR) pulses which originated from the rotor disk to calculate the output pulse frequency required to generate a given number of pulses per revolution. The required frequency was fed to a frequency-agile clock within the encoder which then generated the desired number of clock counts independent of rotor speed drifts. The shaft angle encoder was configured to give 1656 counts per revolution or 46 counts per blade passage. The resulting nominal sampling frequency is shown in Table 2. Each hot wire of the aspirating probe was operated by a separate Dantec model 55M01 constant temperature anemometer.

A careful calibration of the aspirating probe and Kulite was done to minimize calibration uncertainties which would predominately result in bias errors. When only the noise levels of each hot wire signal are taken in account, the corresponding total pressure and total temperature variations calculated are approximately ±1.24 kPa and ±0.80K. For the Kulite, the noise level translates to ±0.20 kPa. For the one-wire/Kulite data, noise results in a ±0.72K temperature band. Hot wire aging, Kulite sensor aging, and Kulite amplifier drift all can cause significant shifts of the instrument calibrations. Since we are presently concerned mainly with the response of the probe to changes in total pressure and temperature, the shifts in the calibrations are not yet a serious problem.

Since the Kulite total pressure sensor was mounted next to the aspirating probe, there was some concern about the impact of angular sensitivity effects on the accuracy of its total pressure measurement. Additionally, laser anemometer measurements indicated large flow angle variations from core flow to wake. Total pressure was therefore measured independently using a Kiel type probe fitted with a Kulite XCQ-062–50A high response pressure transducer. Because of electronic noise this transducer has a resolution of ±0.45 kPa. This probe is insensitive to flow angles up to ±40° as determined in a calibration jet. Pressure measurements were acquired with this Kiel probe at the same axial measurement location as the aspirating probe and adjacent Kulite.

Velocity and flow angle data were acquired using a two-channel laser fringe anemometer (LFA) system. The LFA data have a resolution of 184 points per blade passage and were acquired slightly upstream of the station 3 measurement location. The LFA data from further upstream suggests that negligible wake decay occurred from the LFA measurement location to the aspirating probe measurement location.

The data were averaged using an OPR ensemble averaging method to show flow structure. OPR averaging indexes the averaging by the number of counts per revolution to give information for an average revolution. The data could be further averaged by indexing by the number of counts per blade to give information for an average passage. The pressure probe and aspirating probe data are presented below as three characteristic passages of an average revolution. The LFA data are for an average passage that is repeated three times.

## RESULTS

Measurements were made at the 60% speed operating condition

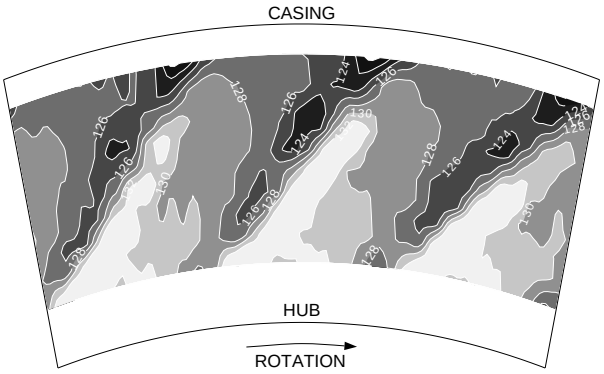


FIGURE 6 Blade to blade view of total pressure (kPa) in three passages at station 3 calculated from the aspirating probe hw1 and hw2 voltages.

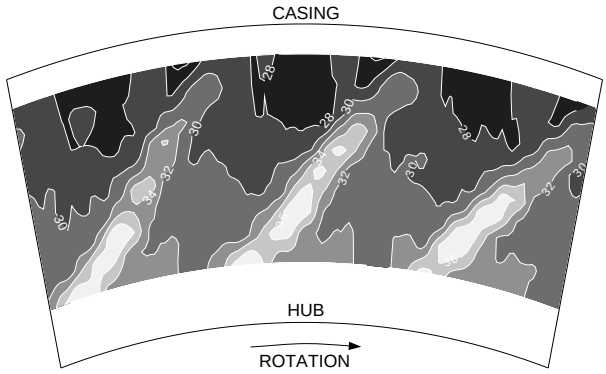


FIGURE 7 Blade to blade view of total temperature (°C) in three passages at station 3 calculated from the aspirating probe hw1 and hw2 voltages.

using the aspirating probe and adjacent Kulite transducer, the high-response Kiel-headed pressure probe, and the LFA system, all at or near station 3. The improved sensitivity of the aspirating probe allowed measurement of pressure and temperature fields using the two hot wire voltages only. The two-wire measured pressure field is compared to that measured using the Kulites mounted on both the aspirating probe and the Kiel-headed probe. In addition, the two-wire measured temperature field is compared to that field calculated with the Euler turbine equation from LFA velocity data and with that field measured with one wire and the adjacent Kulite.

## TWO WIRE RESULTS

Figures 6 and 7 show the blade-to-blade views of the total pressure and total temperature fields measured using the two wire voltages. Three representative blade passages are shown and the annulus boundary is represented as a black border with the upper line being the casing (100% span) and the lower line being the hub (0% span). Contour level increments are consistent throughout all of the figures, however, for better clarity and contrast the contour level shading does not always represent the same contour value between the figures. Each blade wake shows clearly as a region of higher total temperature. The total temperature increases approximately 5.0°C (9°F) above the core flow temperature. This temperature increase corresponds to an increase in total pressure as shown in Figure 6. The total pressure increases approximately 6.9 kPa (1.0 psi) above the core flow pressure. All temperatures and pressures are measured in the absolute reference frame.

As an independent check of the temperature response of the aspirating probe, total temperature was calculated with the Euler turbine equation from the tangential velocities measured with the LFA system. Figure 8 shows the blade-to-blade total temperature contours for an average passage repeated three times. Because of the different circumferential measurement locations of the LFA system and aspirating probe, the blade wakes do not appear in exactly the same circumferential position in Figures 8 and 7. However, the character of the temperature signatures is very similar. The wakes appear narrower in Figure 8 due to the superior spatial resolution of the LFA system. The total temperature difference is

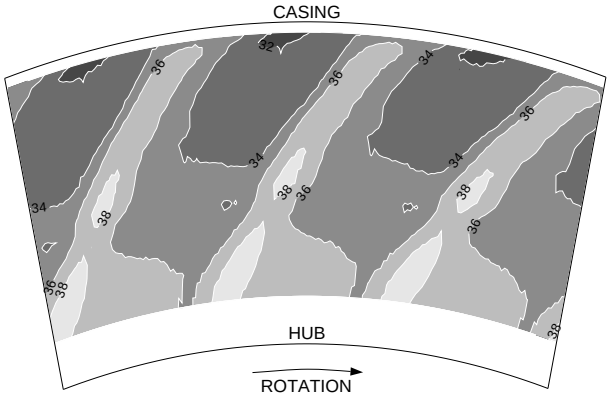


FIGURE 8 Total temperature (°C) contours calculated from LFA velocities near station 3.

approximately 3.3°C (6°F) from core flow to blade wake as compared to 5.0°C (9°F) for the two-wire results. Because the LFA data represent an average passage, the temperature increase in the wake could be attenuated in the averaging process by passage-to-passage flow non-uniformities in the rotor. The absolute levels of total temperature obtained with the aspirating probe and the Euler equation calculations do not match exactly. Absolute value differences like this are caused by aging of the hot wires which causes a 'DC' type shift in the temperatures and pressures calculated from the hot wire voltages. The magnitude of the fluctuations however, are not influenced by wire drift. Because pre- and post-calibrations were not done immediately preceding and following this aspirating probe data set, a standard combination probe $P_T/T_T$ measurement at 30% span was used to help determine wire drift. All aspirating probe hotwire voltages were corrected in post processing so that the average of the two-wire $P_T$ and $T_T$ measurements at 30% span match the standard probe measurement at 30% span. The issue of calibration drift will be addressed in more detail in a following section.

The total pressure data measured with the improved aspirating probe can be compared with the pressure signature measured with the high-response Kiel probe as shown in Figure 9. The blade

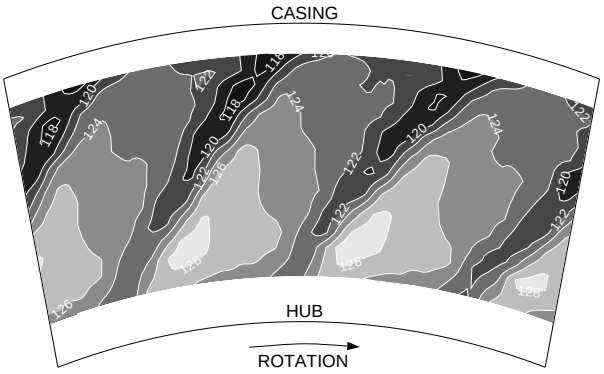


FIGURE 9 Total pressure (kPa) contours at station 3 from the high-response Kiel probe.

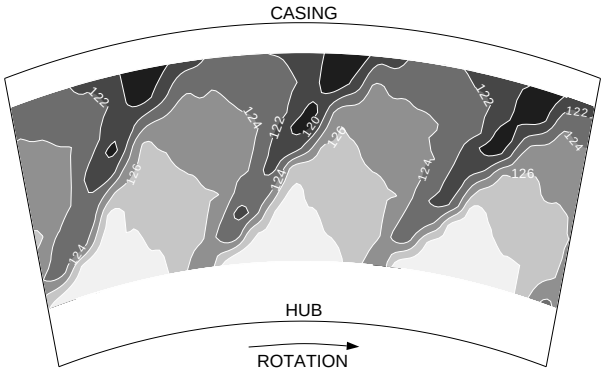


FIGURE 10 Total pressure (kPa) contours at station 3 from the Kulite transducer mounted beside the aspirating probe.

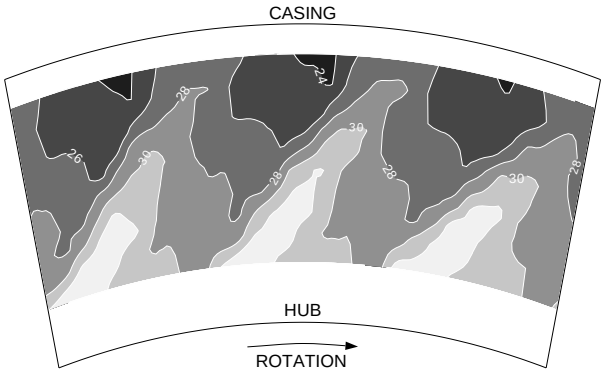


FIGURE 11 Total temperature (°C) contours at station 3 calculated from the Kulite pressure and hot wire 1 voltage.

wakes are shifted circumferentially because of different instrument measurement locations in Figures 6 and 9. The character of the pressure signatures is similar but the pressure transducer shows a variation of only 6.9 kPa (1 psi) from core flow to wake while a 10.2 kPa (1.5 psi) variation is suggested by the aspirating probe. The pressure probe measures the pressure over a larger face area than the aspirating probe and this may account for some of the attenuation of the wake. The absolute level of pressure can also vary because of hot wire aging.

The comparisons with independent instrumentation measurements confirm that the improved aspirating probe is responding adequately to pressure and temperature fluctuations with the two wire voltages only used for data reduction as originally intended. It is now informative to compare the results of earlier data reduction techniques with the results of the two wire method.

## ONE-WIRE/KULITE BASED RESULTS

Because of aspirating probe sensitivity problems, earlier data reduction methods used a total pressure measurement from a Kulite XCQ-062–25G pressure transducer mounted beside the aspirating probe and only one of the hot wire voltages to calculate total temperature. Figures 10 and 11 show the total pressure measured with the Kulite transducer and total temperature field calculated from the Kulite pressure and hot wire 1 voltage.

The character of the pressure contours of Figures 9 and 10 is similar, however, the absolute values of the pressures are different due to amplifier drift and aging of the semiconductor transducers. More frequent calibration of the transducers would have helped reduce these differences. The similarities indicate that the transducer mounted beside the aspirating probe is capturing the total pressure fluctuations and that blockage effects from the proximity of the aspirating probe are not significant for this flow case. While the total pressure measurement is reasonable as expected, the total temperature measurement using only one wire and a pressure transducer is less acceptable.

The total temperature contours of Figure 11 do not have the well defined structure of those obtained with two wires shown in Figure 7. The blade wake appears 'washed out' in Figure 11; the $T_T$ rise in the wake is not as well defined. Figure 12 demonstrates this by showing a comparison of the blade wakes at 30% span as measured with two wires and with one-wire/Kulite. Both temperature signatures had their respective minimum values subtracted. For the one-wire/Kulite results the parameters of wake width and depth are not accurately represented. The two-wire results consistently show a prominent blade wake as anticipated from the LFA measurements. The width and depth of the wake are readily visible. The two-wire measurements are apparently more sensitive to the unsteady total temperature fluctuations and are thus better able to resolve the wake flow.

The total temperature field of Figure 11 is strongly influenced by the total pressure value used to solve Eqn. 8, by the time shift applied to bring the hot wire response and Kulite response into phase with each other, and by the differing frequency response characteristics of the Kulite and the hot wire.

Past experience with data reduction using Kulite pressure and a single hot wire voltage has shown that the resultant total temperature mimics trends in the total pressure signal. The pressure and temperature waveforms follow each other even when the pressure waveform is purposely shifted significantly out of phase with the hot wire signal before data reduction. Data reduction using the Kulite pressure assumes that the pressure signal measured by the Kulite and the pressure signal as calculated from the two wires

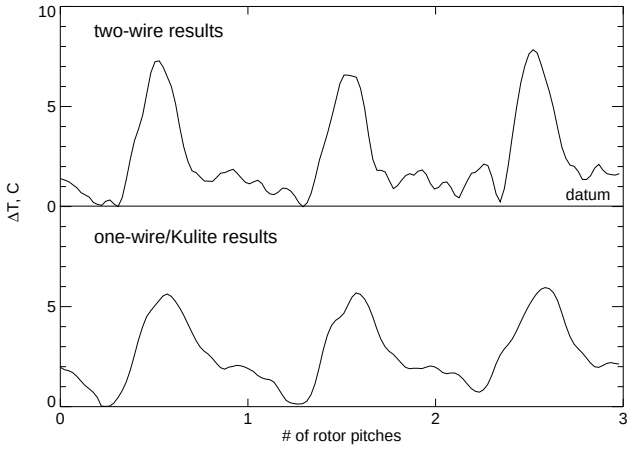


FIGURE 12 Comparison of blade temperature wakes at 30% span.

are identical. Figures 6 and 10 show that the pressure signals are similar but not identical and thus the total temperature calculated by the two-wire and the one-wire/Kulite methods are not the same.

Because the Kulite transducer and aspirating probe are mounted side by side, the spatial separation of these instruments is likely to cause a time shift or lag between the signals. In previous applications the time lag had a negligible effect on the results (Alday et al., 1993). For the improved aspirating probe, the time lag between the Kulite signal and the hot wire signal has a significant effect on the shape of the temperature waveform and on the magnitude of the temperature variations calculated. A cross correlation of the pressure waveform calculated using the two hot wire voltages and the pressure waveform measured with the adjacent Kulite transducer indicated a shift of +2 encoder counts for the Kulite signal relative to the hot wire signals. Thus the first data point of the Kulite signal was reduced with the third point of the hot wire 2 signal to determine a total temperature. This shift is opposite of what is expected due to spatial separation indicating that there is a residence time in the aspirating probe associated with when a change occurs at the face of the probe to when it is sensed at the hot wire plane. Kotidis (1989) found a similar time lag in the signals due to convection time in the aspirating channel.

Well tuned hot-wire anemometers have a frequency response of at least 60 kHz according to the manufacturers specifications. The response of the aspirating probe is limited by the geometry of the aspirating channel. The frequency response of a slightly larger aspirating probe was found to be approximately 20 kHz (Kotidis, 1989). The frequency response of the current size probe has not been experimentally verified but should be at least 20 kHz also (Alday, 1991). The frequency response of the Kulite transducer is influenced by its mounting beside the aspirating probe in a sharp edged recess and the B-screen used to shield the transducer. The manufacturer claims no effect on dynamic response from the B-screen out to 20 kHz. For aerodynamic reasons several researchers expect the response to be less. If the Kulite transducer is not able to adequately resolve the pressure fluctuation though the wake, the total temperature calculated using the Kulite and one hot wire will be compromised. This total temperature signature does not adequately show the structure of the flowfield indicated by the two wire results and the LFA based temperature calculations.

Total temperature data obtained with the Kulite pressure as an input value is inferior to the two wire data. The lack of similarity of Figure 11 compared with Figures 7 and 8 supports this conclusion.

## REMAINING LIMITATIONS

Even with the improved sensitivity of the modified aspirating probe some problems still exist with angle sensitivity, frequency response, and absolute value resolution.

The aspirating probe has a round lip entrance region to improve the acceptance angle range for off axis flows. The probe is insensitive to flow angles up to ±12.5° (Alday, et al., 1993). The data presented in this paper were acquired far downstream of the rotor where flow angle changes between the core flow and wake flow are 5° to 6° according to LFA data. Just downstream of Rotor 37 the flow angle changes across the blade wakes are 30° to 40°. Because of the limited acceptance angle range of the aspirating probe, measurements in the more hostile flow region close to Rotor 37 must be interpreted carefully.

For high speed applications the frequency response of the aspirating probe may not be adequate to resolve unsteady flow phenomena. At 60% speed the blade passing frequency is 6.2 kHz, thus the aspirating probe can capture at least 4 harmonics. The design speed blade passing frequency is 10.3 kHz of which the aspirating probe can capture only 2 harmonics. The LFA system data indicate narrow, well defined triangular-shaped wakes downstream of Rotor 37. The spectral representation of such a waveform requires multiple harmonics and in some applications the aspirating probe may not have the frequency response to capture the necessary harmonics.

Figure 13 shows the flow regimes for past and present applications of the aspirating probe. PW1 and PW2 are Pratt and Whitney fans. W is a Wennerstrom high thru-flow rotor tested in the MIT blowdown facility. R37 and R67 are NASA Rotors 37 and 67. The only total pressure and total temperature measurements obtained with only two wires were acquired downstream of Rotor 37 at part speed operation, the compressor operating condition highlighted in the figure. The other measurements were made with an adjacent pressure probe and only one wire of the aspirating probe. Severe challenges remain in making reliable aspirating probe measurements in the aggressive flow regions close to the exit of high pressure ratio, high-speed rotors.

Because of calibration shifts due to aging of the hot wires, determining absolute values of pressure and temperature is still difficult. The smaller temperature coefficient of resistance of platinum iridium wires makes them more susceptible to this problem than tungsten wires. Small changes in wire resistance will cause large changes in wire temperature. The only way to judge the drift of the wires is to do pre and post test calibrations of the probe to bracket the drift of pressure and temperature values after data acquisition. Hot wire aging should not affect the magnitude of

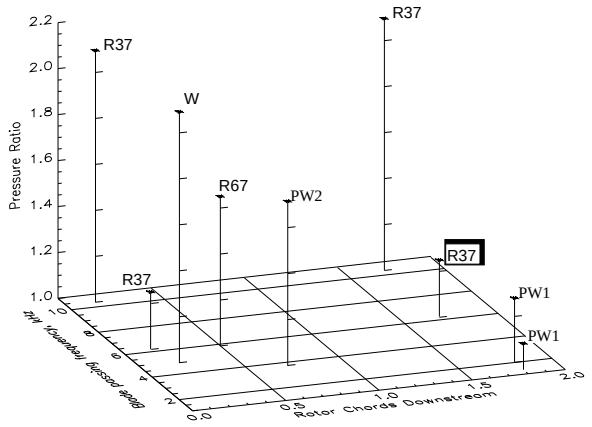


FIGURE 13 Comparison of compressor operating conditions for past and present aspirating probe applications.

the pressure and temperature variations measured by the probe as much as the absolute level of the results.

## SUMMARY

The use of platinum/iridium wires in the aspirating probe has enabled the current researchers to achieve a large difference in the operating temperature of the two wires while simultaneously maintaining a large temperature difference between the wires and the flow field temperature. These temperature characteristics were vital to the successful application of the two-wire technique to aspirating probe data reduction.

Since the aspirating probe calibration constants are functions of total temperature, a calibration must be done that characterizes the range of temperatures and pressures of interest for the experiment. This complete set of calibration information must be incorporated into the data reduction procedure to achieve good results.

Use of the one-wire/Kulite data reduction technique has been required in previous investigations due to temperature limitations which arise when using tungsten hot wires. In the present investigation, unsteady pressure and temperature results were generated with the two-wire technique and compared to those calculated from the same set of measurements with the one-wire/Kulite technique. Comparisons between the two aspirating probe techniques, independent Kulite pressure measurements, and temperatures calculated from laser anemometer measurements indicate that the two-wire technique generates improved results relative to the one-wire/Kulite technique.

An additional benefit resulting from the success of the two-wire technique is that the Kulite pressure transducer which has been piggy-backed onto the aspirating probe in both the present and previous investigations is no longer required. Removal of the Kulite will result in a 50% reduction in the physical size of the aspirating probe head and the resulting flow blockage. Also the problems associated with taking measurements in different meridional planes is eliminated.

Remaining limitations of the aspirating probe include angle sensitivity, frequency response, and absolute value resolution.

## ACKNOWLEDGMENTS

This work was done at the NASA Lewis Research Center under grant number NAG3–1302. We are grateful to Dr. Wing Ng for his useful suggestions and to Dr. David Davis for his help with hot wire concerns.

## REFERENCES

Alday, J., and Ng, W. The correlation of randomness with high tip losses in an axial flow fan stage. Master's thesis, Virginia Polytechnic Institute and State University, Blacksburg, 1991.

Alday, J., Osborne, D. J., Morris, M. B., and Ng, W. Flow randomness and tip losses in transonic rotors. *ASME paper 93–GT-189* (1993).

Boeing Computer Services and United States Navy, Naval Surface Warfare Center, David Taylor Model Basin. *DT_NURBS Spline Geometry Subprogram Library User's Manual*, October 1992.

Cherrett, M., and Bryce, J. Unsteady viscous flow in a high speed core compressor. *Journal of Turbomachinery* (1991), 287–294.

Kotidis, P. A. Unsteady radial transport in a transonic compressor stage. Tech. Rep. GTL #199, Gas Turbine Laboratory, Massachusetts Institute of Technology, September 1989.

Moore, R. D., and Reid, L. Performance of single-stage axial-flow transonic compressor with rotor and stator aspect ratios of 1.19 and 1.26, respectively, and with design pressure ration of 2.05. Tech. rep., NASA TP- 1659, 1980.

Morris, M. B., Osborn, D. J., and Ng, W. F. Flow randomness and tip losses in transonic rotors. Tech. rep., Virginia Polytechnic Institute and State University, Mech. Engr. Dept., May 1992.

Ng, W. *Time-Resolved Stagnation Temperature Measurement in a Transonic Compressor*. PhD thesis, Massachusetts Institute of Technology, Cambridge, October 1983.

Ng, W. F., and Epstein, A. H. High-frequency temperature and pressure probe for unsteady compressible flows. *Review of Scientific Instruments* (December 1983), 1678–1683.

Reid, L., and Moore, R. D. Design and overall performance of four highly loaded, high speed inlet stages for an advanced high-pressure ratio core compressor. Tech. rep., NASA TP- 1337, 1978.

Smits, A., Hayakawa, K., and Muck, K. Constant temperature hot-wire anemometer practice in supersonic flows. *Experiments in Fluids* (1983), 83–92.

Van Zante, D. E. Slow and fast-response instrument flowfield measurements downstream of a transonic axial-flow compressor rotor. Master's thesis, Iowa State University, 1992.

# AN IMPROVED ASPIRATING PROBE FOR TOTAL-TEMPERATURE AND TOTAL-PRESSURE MEASUREMENTS IN COMPRESSOR FLOWS

**Dale E. Van Zante**
Dept. of Mech. Engr.
Iowa State University
Ames, Iowa

**Kenneth L. Suder**
Internal Fluid Mechanics Division
NASA Lewis Research Center
Cleveland, Ohio

**Anthony J. Strazisar**
Internal Fluid Mechanics Division
NASA Lewis Research Center
Cleveland, Ohio

**Theodore H. Okiishi**
Dept. of Mech. Engr.
Iowa State University
Ames, Iowa